Journal of Organometallic Chemistry 694 (2009) 3362–3368

Contents lists available at ScienceDirect

Journal of Organometallic Chemistry

journal homepage: www.elsevier.com/locate/jorganchem

Reactions of half-sandwich rhodium(III) and iridium(III) compounds with pyridinethiolate ligands: Mono-, di-, and tri-nuclear complexes

Hui Wang, Xu-Qing Guo, Rui Zhong, Yue-Jian Lin, Peng-Cheng Zhang, Xiu-Feng Hou *

Department of Chemistry, Fudan University, Han Dan Road 220, Shanghai 200433, People's Republic of China

ARTICLE INFO

Article history:
Received 21 April 2009
Received in revised form 21 May 2009
Accepted 26 May 2009
Available online 3 June 2009

Keywords:
Rhodium
Iridium
Pyridinethiolate
Mononuclear
Dinuclear
Trinuclear

ABSTRACT

Neutral trinuclear metallomacrocycles, $[Cp^*RhCl(\mu\text{-}4\text{-}PyS)]_3$ (**3**) and $[Cp^*IrCl(\mu\text{-}4\text{-}PyS)]_3$ (**4**) [Cp^* = pentamethylcyclopentadienyl, 4-PyS = 4-pyridinethiolate], have been synthesized by self-assembly reactions of $[Cp^*RhCl_2]_2$ (**1**) and $[Cp^*IrCl_2]_2$ (**2**) with lithium 4-pyridinethiolate, respectively. In situ reaction of complex **3** with three equivalent of lithium 4-pyridinethiolate resulted in $[Cp^*Rh(\mu\text{-}4\text{-}PyS)(4\text{-}PyS)]_3$ (**5**) containing both skeleton and pendent 4-PyS groups. Chelating coordination of 2-pyridinethiolate broke down the triangular skeleton to give mononuclear metalloligands $Cp^*Rh(2\text{-}PyS)(4\text{-}PyS)$ (**6**) and $Cp^*Ir(2\text{-}PyS)(4\text{-}PyS)$ (**7**) [2-PyS = 2-pyridinethiolate], which could also be synthesized from $Cp^*RhCl(2\text{-}PyS)$ (**10**) and $Cp^*IrCl(2\text{-}PyS)$ (**11**) with lithium 4-pyridinethiolate. The coordination reactions of **6** with complexes **1** and **2** gave dinuclear complexes $[Cp^*Rh(2\text{-}PyS)(\mu\text{-}4\text{-}PyS)][Cp^*RhCl_2]$ (**8**) and $[Cp^*Rh(2\text{-}PyS)(\mu\text{-}4\text{-}PyS)][Cp^*IrCl_2]$ (**9**), respectively. Molecular structures of **3**, **4**, **6** and **11** were determined by X-ray crystallographic analysis. All the complexes have been well characterized by elemental analysis, NMR and IR spectra.

1. Introduction

The coordination chemistry of pyridinethiolate ligands is of great importance in a variety of reactions [1], due to the unusual coordination geometry, variety of bonding, and interesting spectral and electrochemical behavior of these complexes [2–4]. The products of such ligands with metal atoms are found to have special properties for many applications, such as, antitumor potential with gold and platinum [5], dimerization catalyst of alkynes with iridium [6], vitro potency against trypanozoma cultures with tin [7], and control of the behavior of nucleic acids as tautomeric systems [8]. However, the half-sandwich complexes, which have cobalt, rhodium, or iridium centers with the pyridinethiolate ligands, are still under comprehensive investigation [9,10]. In our previous work, we reported the reactivity of half-sandwich Cp^*Co complexes with 1,2-dicarba-*closo*-dodecaborane (12)-1,2-dithiolato ligand, pyridinethione ligand, heterocyclic thione ligand and benzenethiolate ligand [11–13].

In this paper, we would like to communicate on the reactivity of half-sandwich Cp^*Rh or Cp^*Ir complexes towards pyridinethiolate. Mono-, di-, and tri-nuclear organometallic compounds are described.

2. Results and discussion

2.1. Self-assembly reactions of *1* and *2* with 4-pyridinethiolate

The treatment of $[Cp^*RhCl_2]_2$ (**1**) with two equivalent of lithium pyridine-4-thiolate in THF afforded $[Cp^*RhCl(\mu\text{-}4\text{-}PyS)]_3$ (**3**) as a red solid in moderate yield (Scheme 1). Complex **3** is air stable, and soluble in THF and CH_2Cl_2. The ^1H NMR spectrum of **3** shows three signals for the ring-methyl groups of C_5Me_5 (δ 1.43, 1.41, 1.39), which is indicative of unsymmetrical cyclic structure.

Crystals of complex **3** were obtained by slow diffusion of hexane into a concentrated solution of the complex in dichloromethane at low temperature. The structure of complex **3** crystallizes as an approximately equilateral triangle with Rh(1)···Rh(2), Rh(2)···Rh(3) and Rh(3)···Rh(1) distances of 8.157, 8.098, and 8.083 Å, respectively, which means a *C*1 structure. By now, only a few half-sandwich organometallic triangular complexes have been explored [14–24], in which using bridging ligands with S and N as coordinating atoms are extremely rare. As depicted in Fig. 1a, the molecular structure consists of alternating Cp^*Rh vertices and pyridine-4-thiolate edges. For the Cp^*Rh half-sandwich tripod moiety, two of the three "legs" are S and N atoms from two different pyridine-4-thiolato bridges, and the third one is a chlorine atom. The angles between three "legs" are around 90° (N(3)–Rh(1)–S(1) = 93.1(2)°, N(3)–Rh(1)–Cl(1) = 88.3 (2)°, Cl(1)–Rh(1)–S(1) = 96.46(8)°). Here, the C–S–Rh angles are less than 120° (117.4(3)°, 115.0(3)° and 113.8(3)° for C(3)–S(1)–Rh(1), C(8)–S(2)–Rh(2) and

* Corresponding author. Tel.: +86 21 55664007; fax: +86 21 65641740.
E-mail address: xfhou@fudan.edu.cn (X.-F. Hou).

0022-328X/$ - see front matter © 2009 Elsevier B.V. All rights reserved.
doi:10.1016/j.jorganchem.2009.05.034

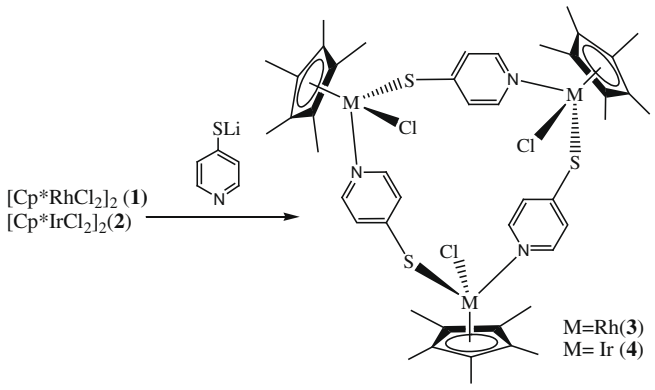

Scheme 1. Synthesis of complex **3** and **4**.

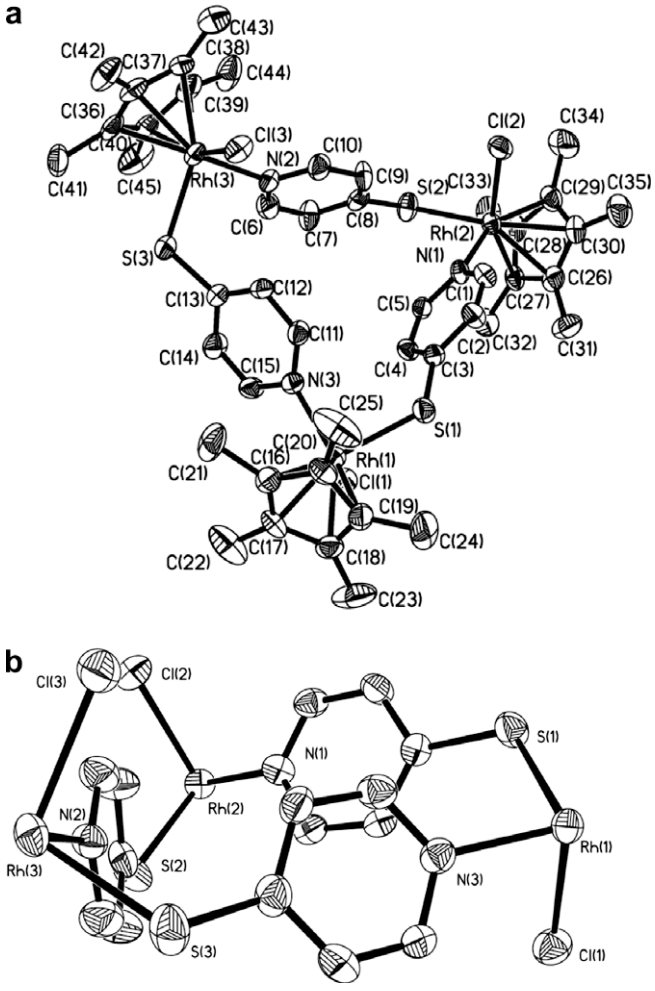

Fig. 1. Molecular structure of **3**, ellipsoids at the 30% probability level. H atoms are omitted for clarity. (a) Global view. (b) Side view (the Cp^* groups have been omitted for clarity). Selected bond lengths (Å) and angles (°): Rh(1)–Cl(1) 2.406(2), Rh(1)–N(3) 2.120(6), Rh(1)–S(1) 2.362(2), S(1)–C(3) 1.737(8). N(3)–Rh(1)–S(1) 93.1(2), N(3)–Rh(1)–Cl(1) 88.3 (2), Cl(1)–Rh(1)–S(1) 96.46(8), Rh(1)–S(1)–C(3) 117.4(3).

C(13)–S(3)–Rh(3), respectively), which appears to be crucial to the formation of the molecular triangle. The Rh–N and Rh–S interactions are slightly out of the trirhodium plane (Fig. 1b). Interestingly, the three chlorine atoms are in different fashion to the plane (two-up, one-down), which makes the 4-PyS group between the two-up ones a little different. That is, from the trirhodium plane, the angle to this 4-PyS unit is 86.3°, while the other two are 76.7° and 72.2°. Another interesting feature of **3** is its packing pattern. As illustrated in Fig. 2, there are triangular channels running along the *a*-axis.

The reaction of $[Cp^*IrCl_2]_2$ (**2**) with lithium pyridine-4-thiolate in THF afforded $[Cp^*IrCl(\mu\text{-}4\text{-}PyS)]_3$ (**4**) as an orange solid in 52% yield. The X-ray crystallographic analysis reveals that, the molecular structure of **4** is similar to the rhodium complex **3**, except that the rhodium atoms are replaced by the iridium atoms (Fig. 3). And the Ir···Ir distances are 8.173, 8.110 and 8.148 Å, respectively, which are a little longer than the Rh···Rh distances. Besides, there are CH_2Cl_2 molecules found outside the triangular channels in the crystal structure of $\mathbf{4}\cdot CH_2Cl_2$. A similar Ir complex was very recently published by Han et al. [25].

2.2. In situ reactions of complex *3* with 4-pyridinethiolate or 2-pyridinethiolate

Since there were residual chlorine atoms in the trinuclear metallomacrocycle, we realized that useful functional groups could be induced by replacing the Cl atoms in situ. Treating complex **3** with three equivalent of lithium pyridine-4-thiolate in THF afforded $[Cp^*Rh(\mu\text{-}4\text{-}PyS)(4\text{-}PyS)]_3$ (**5**) as a red solid in moderate yield (Scheme 2).

The ^{1}H NMR spectrum of **5** also shows three signals for the ring-methyl groups of C_5Me_5 (δ 1.43, 1.42, 1.40) just like that of its starting complex **3**. In the ^{13}C NMR spectrum, there are two groups of signals between 150 and 120 ppm. Signals at δ 149.90, 143.58, 128.05 for the suspending PyS groups show stronger intensity than signals for the skeleton μ-PyS groups at δ 148.70, 127.11, 120.04. So, complex **5** has a similar structure with **3**, in which three chlorine atoms are replaced by three pyridine-4-thiolato groups.

When we brought 2-pyridinethiolate ligand into our triangle **3**, we got red crystals **6** in high yield (Scheme 3). In the ^{1}H NMR spectrum of **6**, four different signals at 8.03, 7.21, 6.69, 6.67 ppm are very close to those of complex **10** in our early work [11], showing that the metal center of **6** coordinates to one 2-PyS ligand in bidentate mode. Another two signals at 8.58 and 7.81 ppm, which are identified as the hydrogen atoms of the 4-PyS ligand, were also detected obviously. All these data suggested that the chelating coordination mode of 2-pyridinethiolate took a priority, breaking down the triangular skeleton, which were consistent with the structure established by X-ray diffraction.

Single crystals of complex **6** were cultivated from CH_2Cl_2/hexane system. Its crystallographic structure (Fig. 4) shows that the two different pyridine circles are at the same side from the S(1)–Rh(1)–S(2) plane. Because of the different coordination modes, Rh(1)–S(1) distance (2.551(5) Å) is longer than Rh(1)–S(2) (2.214(5) Å). The Rh(1)–S(2)–C(6) angle is 107.4(6)° here, leaving the N atom of 4-pyridinethiolate ligand away from the metal center, which shows the potential metalloligand role of **6**.

The similar reaction using complex **4** instead of **3** gave Cp^*Ir(2-PyS)(4-PyS) (**7**) as an orange solid. In the ^{1}H NMR spectrum, 8.20, 7.20, 6.73, 6.58 ppm for 2-PyS ligand and 8.48, 7.80 ppm for 4-PyS ligand, together with other detailed analysis of the spectroscopic data (^{13}C NMR and IR spectra), show that complex **7** has a same structure with complex **6**.

2.3. Coordination reactions of metalloligand *6* with *1* and *2*

With the metalloligand **6** in hand, we tried its coordinating ability with the half-sandwich iridium(III) and rhodium(III) fragments **1** and **2** (Scheme 4).

The coordination reaction of metalloligand **6** with complex **1** in CH_2Cl_2, after recrystallized in CH_2Cl_2/hexane system, gave dinucle-

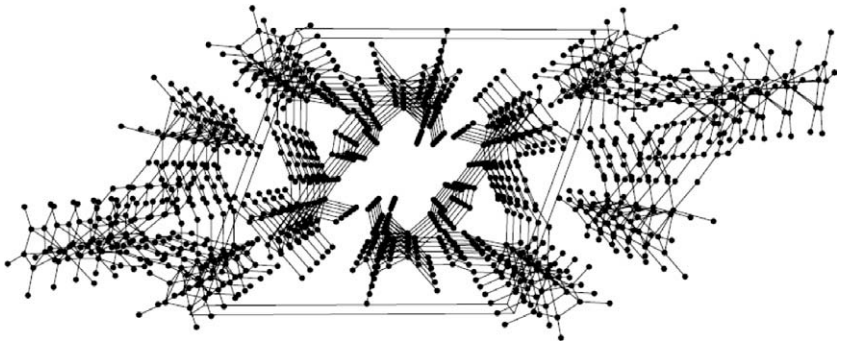

Fig. 2. Crystal structures of **3**, viewed from the *a*-axis.

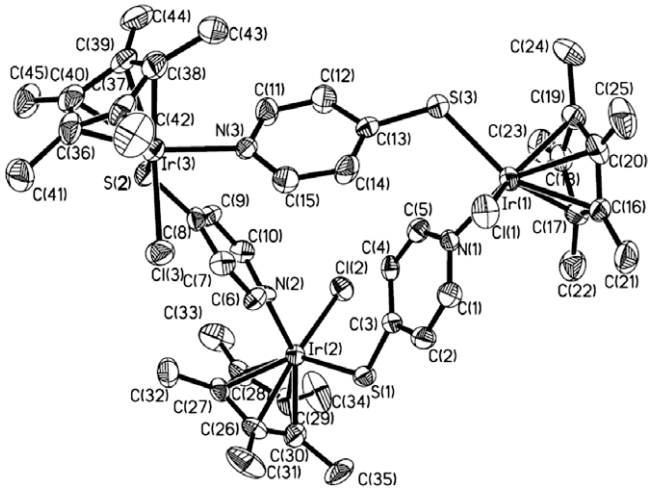

Fig. 3. Molecular structure of **4**, ellipsoids at the 30% probability level. H atoms and solvent molecules are omitted for clarity. Selected bond lengths (Å) and angles (°): Ir(1)–Cl(1) 2.435(3), Ir(1)–N(1) 2.115(9), Ir(1)–S(3) 2.353(4), S(3)–C(13) 1.729(12). N(1)–Ir(1)–S(3) 90.3(3), N(1)–Ir(1)–Cl(1) 88.2(3), Cl(1)–Ir(1)–S(3) 96.6(1), Ir(1)–S(3)–C(13) 115.4(4).

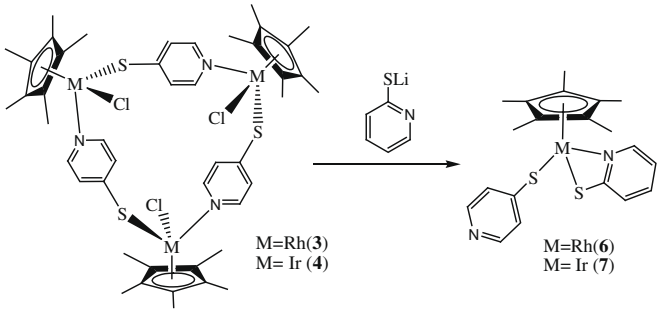

Scheme 3. Synthesis of complex **6** and **7**.

ar compound [$Cp^*Rh(2\text{-}PyS)(\mu\text{-}4\text{-}PyS)$][$Cp^*RhCl_2$] (**8**) as red crystals in 79% yield. Similar peaks can be identified in the ^1H NMR spectrum of the 2-PyS and μ-4-PyS region as complex **6**. And in particular, we found two kinds of peaks appeared at 1.73 and 1.83 ppm, which could be assigned to the two Cp^* groups.

The hetero-nuclear complex **9** could also be synthesized as orange crystals in a same way. The solubility of this compound in common organic solvent is not as good as its analog **8**, which influenced its yield as only 56%.

2.4. Another method to get metalloligands *6* and *7*

Since we got complex **6** from the reaction of starting material **1** with 4-pyridinethiolate to give triangle **3** and then with 2-pyridinethiolate ligand, we believed that it could also be synthesized if we changed the reaction order of these two pyridinethiolate ligands.

As we had already got complex **10** in our early work [11], we used it to react with 4-pyridinethiolate ligand directly (Scheme 5). When the complex **10** reacted with one equiv of the lithium salt of 4-pyridinethione in THF at −78 °C, 4-PyS ligand replaced the chlorine atom to give the red product $Cp^*Rh(2\text{-}PyS)(4\text{-}PyS)$ (**6**) in high yield. Its structure was confirmed by ^1H NMR.

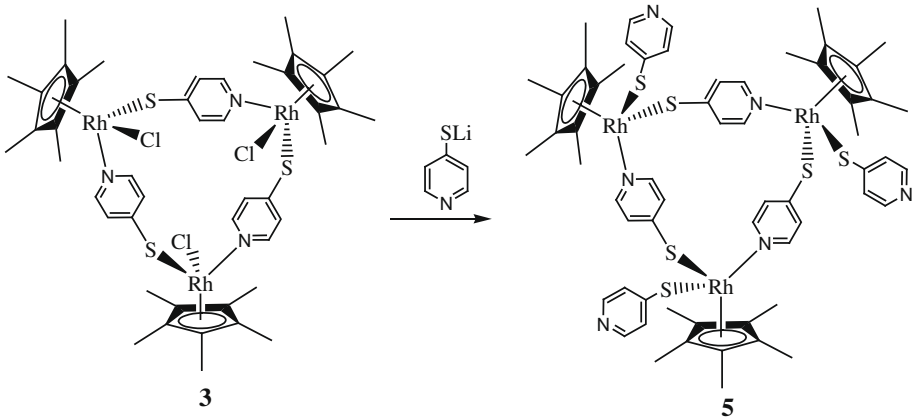

Scheme 2. Synthesis of complex **5**.

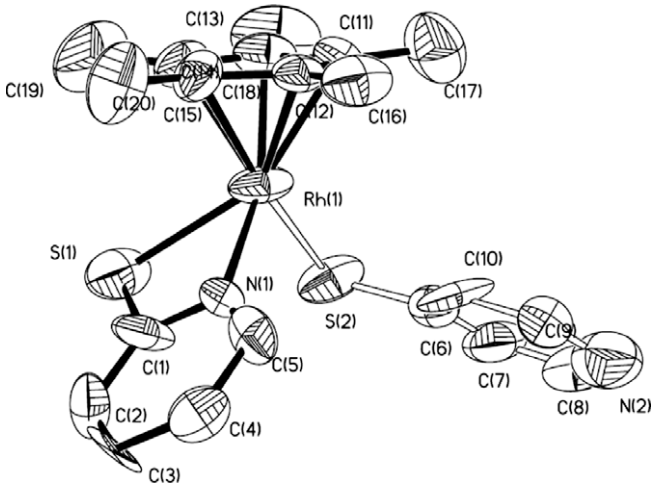

Fig. 4. Molecular structure of **6**, ellipsoids at the 30% probability level. H atoms are omitted for clarity. Selected bond lengths (Å) and angles (°): Rh(1)–N(1) 2.22(1), Rh(1)–S(1) 2.551(5), Rh(1)–S(2) 2.214(5), N(1)–C(5) 1.359(8), N(1)–C(1) 1.359(8), S(1)–C(1) 1.71(1), S(2)–C(6) 1.74(1); N(1)–Rh(1)–S(1) 63.9(4), N(1)–Rh(1)–S(2) 91.8(3), S(1)–Rh(1)–S(2) 86.8(2), N(1)–C(1)–S(1) 111.3(9), C(6)–S(2)–Rh(1) 107.7(6).

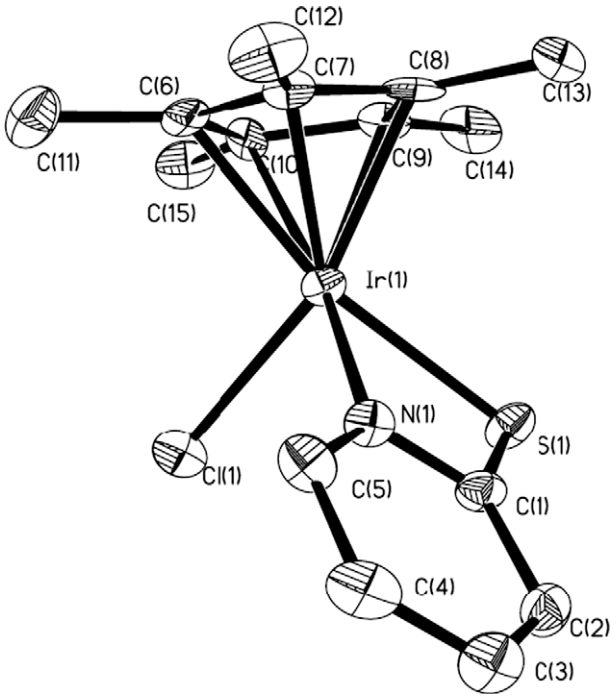

Fig. 5. Molecular structure of **11**, ellipsoids at the 30% probability level. H atoms are omitted for clarity. Selected bond lengths (Å) and angles (°): Ir(1)–N(1) 2.107(10), Ir(1)–S(1) 2.419(3), Ir(1)–Cl(1) 2.401(3), N(1)–C(5) 1.319(15), N(1)–C(1) 1.340(14), S(1)–C(1) 1.726(12); N(1)–Ir(1)–S(1) 67.0(3), N(1)–Ir(1)–Cl(1) 84.2(3), S(1)–Ir(1)–Cl(1) 90.43(13), N(1)–C(1)–S(1) 109.4(8).

Following this route, the reaction of 2-pyridinethione with one equivalent of *n*-BuLi, followed by addition of one equivalent of $[Cp^*IrCl_2]_2$ (**2**) in THF gave complex Cp^*IrCl(2-PyS) (**11**) as an orange solid (Scheme 5). The crystallographic structure (Fig. 5) shows that complex **11** possesses a half-sandwich tripod structure, with 2-PyS ligand chelating to the metal center in a N, S-bidentate mode. The reaction of complex **11** with lithium pyridine-4-thiolate gave metalloligand **7** in the yield of 64%.

3. Conclusions

In this article, we have described a simple and efficient method to synthesize trinuclear half-sandwich iridium(III) and rhodium(III) macrocycles ($[Cp^*IrCl(\mu\text{-}4\text{-}PyS)]_3$ (**3**) and $[Cp^*RhCl(\mu\text{-}4\text{-}PyS)]_3$ (**4**) with bidentate ligand pyridine-4-thiolate. In these two complexes, all the C–S–M angles are between 110° and 120°, which is crucial to the formation of the molecular triangles. And the residual chlorine atoms could be used to bring in useful functional groups by in situ replacement reactions, such as pyridine-4-thiolate to get complex $[Cp^*Rh(\mu\text{-}4\text{-}PyS)(4\text{-}PyS)]_3$ (**5**). Bringing in 2-pyridinethiolate ligand would destroy the triangular structure to give mononuclear metalloligands Cp^*Rh(2-PyS)(4-PyS) (**6**) and Cp^*Ir(2-PyS)(4-PyS) (**7**). In these two complexes, 2-pyridinethiolate seizes two coordinating sites as a chelating ligand and 4-pyridin-

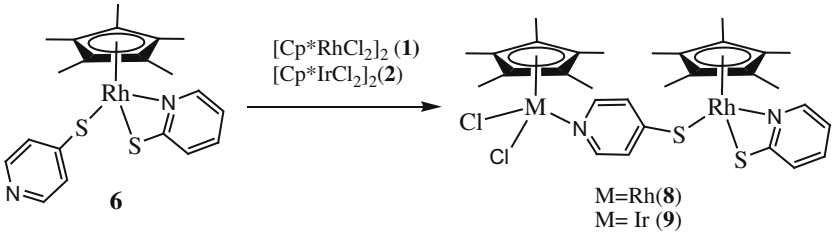

Scheme 4. Synthesis of complex **8** and **9**.

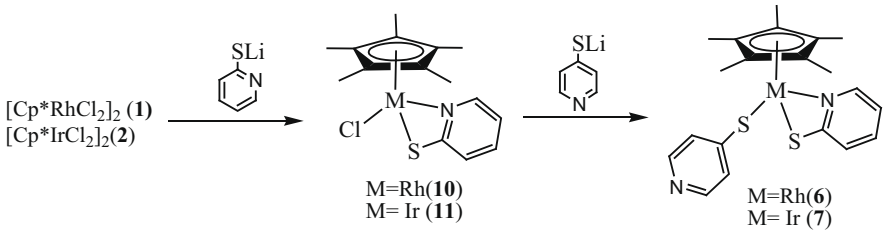

Scheme 5. Synthesis of complex **6** and **7** through **10** and **11**.

ethiolate adopts a monodentate mode with S atom, leaving pyridine N atom away from the metal center. The coordination reactions of **6** with $[Cp^*RhCl_2]_2$ (**1**) and $[Cp^*IrCl_2]_2$ (**2**) give dinuclear complexes **8** and **9** in high yield. The complexes **3**, **4**, **5**, **6** and **7** are useful derivatives for further investigations.

4. Experimental

4.1. General procedures

All reactions and manipulations were carried out using standard Schlenk techniques under nitrogen atmosphere. Solvents were dried and deoxygenated by M. Braun Solvent Purification System (4464) and collected just before use. $[Cp^*RhCl_2]_2$ [26] and $[Cp^*IrCl_2]_2$ [26] were prepared according to the procedures described in the literature. 2-Mercaptopyridine and 4-mercaptopyridine were used as purchased without further purifications. The element analyses were performed on Elementar III Vario EI Analyzer. Infrared spectra were recorded on a Nicolet AVATAR-360IR spectrometer. ^1H NMR (500 MHz) and ^{13}C NMR (125 MHz) spectra were obtained using Bruker DMX-500 spectrophotometer in $CDCl_3$, respectively.

4.2. Preparation of $[Cp^*RhCl(\mu\text{-}4\text{-}PyS)]_3$ (**3**)

A solution of *n*-BuLi (1.6 M, 0.32 ml, 0.5 mmol) in hexane was added dropwise to a solution of 4-mercaptopyridine (55 mg, 0.5 mmol) in 8 ml of THF at 0 °C. The suspension was stirred for another 1 h at room temperature. Then the solution was slowly added to a solution of $[Cp^*RhCl_2]_2$ (155 mg, 0.25 mmol) in THF (20 ml) at −78 °C. After it had been stirred for one day, the solvent was removed under reduced pressure, and the residue was extracted with CH_2Cl_2. The filtrate was concentrated to about 5 ml and hexane was added, to give **3** as a red solid. Yield: 146 mg, 76%. Anal. Calc. for $C_{45}H_{57}N_3Rh_3Cl_3S_3$: C, 46.95; H, 4.99; N, 3.65. Found: C, 46.90; H, 5.04; N, 3.61%. ^1H NMR (500 MHz, $CDCl_3$, ppm): δ 8.61 (d, 3H, μ-4-PyS), 7.74 (d, 3H, μ-4-PyS), 1.43 (s, 15H, Cp^*), 1.41 (s, 15H, Cp^*), 1.39 (s, 15H, Cp^*). ^{13}C NMR (125 MHz, $CDCl_3$, ppm): δ 149.29, 129.05, 120.01 (μ-4-PyS), 95.47, 95.43, 95.40, 9.20, 9.16, 9.01 (Cp^*). IR (KBr disk): ν = 2962, 2918, 2847, 1587, 1462, 1378, 1261, 1103, 1023, 803, 729, 508 cm^{-1}.

4.3. Preparation of $[Cp^*IrCl(\mu\text{-}4\text{-}PyS)]_3$ (**4**)

The procedure is similar to the preparation of complex **3**. Using *n*-BuLi (1.6 M, 0.32 ml, 0.5 mmol), 4-mercaptopyridine (55 mg, 0.5 mmol) and $[Cp^*IrCl_2]_2$ (200 mg, 0.25 mmol) to give **4** as an orange solid. Yield: 123 mg, 52%. Anal. Calc. for $C_{45}H_{57}N_3Ir_3Cl_3S_3$: C, 38.05; H, 4.05; N, 2.96. Found: C, 38.11; H, 4.03; N, 2.91%. ^1H NMR (500 MHz, $CDCl_3$, ppm): δ 8.76 (d, 6H, μ-4-PyS), 7.90 (d, 6H, μ-4-PyS), 1.42 (s, 15H, Cp^*), 1.41 (s, 15H, Cp^*), 1.39(s, 15H, Cp^*). ^{13}C NMR (125 MHz, $CDCl_3$, ppm): δ 149.29, 128.49, 119.22 (PyS), 90.69, 90.15, 87.48, 9.00, 8.55, 8.51 (Cp^*). IR (KBr disk): ν = 2962, 2921, 2852, 1592, 1464, 1377, 1261, 1102, 1023, 803, 731, 702, 502 cm^{-1}.

4.4. Preparation of $[Cp^*Rh(\mu\text{-}4\text{-}PyS)(4\text{-}PyS)]_3$ (**5**)

A solution of *n*-BuLi (1.6 M, 0.08 ml, 0.12 mmol) in hexane was added dropwise to a solution of 4-mercaptopyridine (13 mg, 0.12 mmol) in 8 ml of THF at 0 °C. The suspension was stirred for another 1 h at room temperature. Then the solution was slowly added to a solution of $[Cp^*RhCl(4\text{-}PyS)]_3$ (**3**) (46 mg, 0.04 mmol) in THF (15 ml) at −78 °C. After it had been stirred at room temperature for one day, the solvent was removed under reduced pressure, and the residue was extracted with CH_2Cl_2. The filtrate was concentrated to about 5 ml and hexane was added, to give **5** as a red solid. Yield: 29 mg, 53%. Anal. Calcd for $C_{60}H_{69}N_6Rh_3S_6$: C, 52.40; H, 5.06; N, 6.11. Found: C, 52.34; H, 5.10; N, 6.06%. ^1H NMR (500 MHz, $CDCl_3$, ppm): δ 8.68 (d, 6H, μ-4-PyS), 7.73 (d, 6H, μ-4-PyS), 8.51 (d, 6H, 4-PyS), 7.37 (d, 6H, 4-PyS), 1.43 (s, 15H, Cp^*), 1.42 (s, 15H, Cp^*), 1.40 (s, 15H, Cp^*). ^{13}C NMR (125 MHz, $CDCl_3$, ppm): δ 149.90, 143.58, 128.05 (4-PyS), 148.70, 127.11, 120.04 (μ-4-PyS), 98.94, 98.89, 98.62, 8.59, 8.23, 8.06 (Cp^*). IR (KBr disk): ν = 2963, 2910, 2853, 1613, 1586, 1561, 1460, 1383, 1262, 1102, 1020, 804, 729, 700, 505 cm^{-1}.

4.5. Preparation of $Cp^*Rh(2\text{-}PyS)(4\text{-}PyS)$ (**6**)

Method A. A solution of *n*-BuLi (1.6 M, 0.13 ml, 0.2 mmol) in hexane was added dropwise to a solution of 2-mercaptopyridine (22 mg, 0.2 mmol) in 8 ml of THF at 0 °C. The suspension was stirred for another 1 h at room temperature. Then the solution was slowly added to a solution of $[Cp^*RhCl(4\text{-}PyS)]_3$ (**3**) (77 mg, 0.067 mmol) in THF (15 ml) at −78 °C. After it had been stirred for one day, the solvent was removed under reduced pressure, and the residue was extracted with CH_2Cl_2. The filtrate was concentrated to about 5 ml and hexane was added, to give **6** as a red solid. Yield: 63 mg, 69%.

Method B. A solution of *n*-BuLi (1.6 M, 0.13 ml, 0.2 mmol) in hexane was added dropwise to a solution of 4-mercaptopyridine (22 mg, 0.2 mmol) in 8 ml of THF at 0 °C. The suspension was stirred for another 1 h at room temperature. Then the solution was slowly added to a solution of $Cp^*RhCl(2\text{-}PyS)$ (**10**) (77 mg, 0.2 mmol) in THF (15 ml) at −78 °C. After it had been stirred for one day, the solvent was removed under reduced pressure, and the residue was extracted with CH_2Cl_2. The filtrate was concentrated to about 5 ml and hexane was added, to give **6** as a red solid. Yield: 74 mg, 81%.

Anal. Calc. for $C_{20}H_{23}N_2RhS_2$: C, 52.40; H, 5.06; N, 6.11. Found: C, 52.35; H, 5.11; N, 6.08%. ^1H NMR (500 MHz, $CDCl_3$, ppm): δ 8.58 (d, 2H, 4-PyS), 7.81 (d, 2H, 4-PyS), 8.03 (d, 1H, 2-PyS), 7.21 (t, 1H, 2-PyS), 6.69 (t, 1H, 2-PyS), 6.67 (d, 1H, 2-PyS), 1.73(s, 15H, Cp^*). ^{13}C NMR (125 MHz, $CDCl_3$, ppm): δ 167.98, 147.01, 127.42 (4-PyS), δ 178.68, 146.45, 135.45, 127.52, 116.85 (2-PyS), 95.54, 9.51 (Cp^*). IR (KBr disk): ν = 2958, 2918, 2851, 1569, 1449, 1420, 1261, 1101, 1020, 809, 760, 706, 500 cm^{-1}.

4.6. Preparation of $Cp^*Ir(2\text{-}PyS)(4\text{-}PyS)$ (**7**)

The procedure is similar to the preparation of complex **6**.

Method A. Using *n*-BuLi (1.6 M, 0.13 ml, 0.2 mmol), 2-mercaptopyridine (22 mg, 0.2 mmol) and $[Cp^*IrCl(4\text{-}PyS)]_3$ (**4**) (95 mg, 0.067 mmol) to give **7** as an orange solid. Yield: 56 mg, 51%.

Method B. Using *n*-BuLi (1.6 M, 0.13 ml, 0.2 mmol), 4-mercaptopyridine (22 mg, 0.2 mmol) and $Cp^*IrCl(2\text{-}PyS)$ (**11**) (95 mg, 0.2 mmol) to give **7** as an orange solid. Yield: 70 mg, 64%.

Anal. Calc. for $C_{20}H_{23}N_2IrS_2$: C, 43.80; H, 4.23; N, 5.11. Found: C, 43.76; H, 4.20; N, 5.16%. ^1H NMR (500 MHz, $CDCl_3$, ppm): δ 8.48 (d, 2H, 4-PyS), 7.80 (d, 2H, 4-PyS), 8.20 (d, 1H, 2-PyS), 7.20 (t, 1H, 2-PyS), 6.73 (t, 1H, 2-PyS), 6.58 (d, 1H, 2-PyS), 1.80 (s, 15H, Cp^*). ^{13}C NMR (125 MHz, $CDCl_3$, ppm): δ 164.98, 151.02, 128.78 (4-PyS), δ 179.52, 145.95, 134.48, 129.44, 116.76 (2-PyS), 92.37, 9.47 (Cp^*). IR (KBr disk): ν = 2980, 2959, 2913, 1591, 1445, 1423, 1264, 1111, 1027, 815, 759, 734, 494 cm^{-1}.

4.7. Preparation of $[Cp^*Rh(2\text{-}PyS)(\mu\text{-}4\text{-}PyS)][Cp^*RhCl_2]$ (**8**)

Complex **6** (23 mg, 0.05 mmol) and **1** (15 mg, 0.025 mmol) in CH_2Cl_2 (15 ml) was stirred for 12 h at room temperature. The solvent was concentrated to about 3 ml and hexane was added, to

Table 1
Crystallographic data for compounds **3**, **4**·CH_2Cl_2, **6** and **11**.

	3	**4**·CH_2Cl_2	**6**	**11**
Empirical formula	$C_{45}H_{57}Cl_3N_3Rh_3S_3$	$C_{46}H_{59}Cl_5Ir_3N_3S_3$	$C_{20}H_{23}N_2RhS_2$	$C_{15}H_{19}ClIrNS$
Formula weight	1151.2	1503.99	458.43	473.02
Crystal system	Triclinic	Triclinic	Orthorhombic	Monoclinic
Space group	$P\bar{1}$	$P\bar{1}$	*Pnma*	$P2(1)/c$
a (Å)	8.775(3)	8.826(2)	11.215(5)	12.620(8)
b (Å)	17.390(6)	17.371(5)	17.455(7)	7.684(5)
c (Å)	18.549(6)	18.512(5)	10.273(4)	16.184(10)
α (°)	110.181(5)	110.211(4)	90	90
β (°)	94.324(5)	94.183(4)	90	91.666(8)
γ (°)	90.304(5)	90.071(4)	90	90
Volume (Å^3)	2647.8(15)	2655.3(12)	2010.9(14)	1568.7(17)
Z	2	2	4	4
$F(0\,0\,0)$	1164	1440	936	904
Crystal size (mm)	0.15 × 0.10 × 0.08	0.12 × 0.08 × 0.08	0.15 × 0.10 × 0.06	0.30 × 0.25 × 0.15
θ Range (°)	1.25–27.18	1.39–27.14	2.30–27.15	1.61–25.01
D_{calc} (Mg m^{-3})	1.444	1.881	1.514	2.003
μ (mm^{-1})	1.225	7.902	1.062	8.801
Number of reflections collected	12932	13469	9202	6199
Number of independent reflections	10949	11360	2248	2759
R_{int}	0.0415	0.042	0.0712	0.0986
Number of data/restraints/parameters	10949/0/527	11360/1/541	2248/18/162	2759/0/178
Goodness-of-fit (GOF) on F^2	0.852	0.927	1.142	1.038
R Indices($I > 2\sigma(I)$)[a]	R_1 = 0.0644	R_1 = 0.0608	R_1 = 0.0633	R_1 = 0.0700
	wR_2 = 0.1273	wR_2 = 0.1313	wR_2 = 0.1335	wR_2 = 0.1769
R indices (all data)	R_1 = 0.1270	R_1 = 0.1222	R_1 = 0.1250	R_1 = 0.0779
	wR_2 = 0.1431	wR_2 = 0.1530	wR_2 = 0.1436	wR_2 = 0.1845
Largest difference in peak and hole (e Å^{-3})	1.229 and −0.440	2.209 and −1.047	0.410 and −0.617	4.681 and −4.348

[a] $R_1 = \sum||F_o|-|F_c||/\sum|F_o|$; $R_w = [\sum w(|F_o^2|-|F_c^2|)^2/\sum w|F_o^2|^2]^{1/2}$.

give **8** as a red solid. Yield: 30 mg, 79%. Anal. Calc. for $C_{30}H_{38}N_2Rh_2Cl_2S_2$: C, 47.00; H, 5.00; N, 3.66. Found: C, 46.94; H, 5.08; N, 3.64%. ^{1}H NMR (500 MHz, $CDCl_3$, ppm): δ 8.50 (d, 2H, μ-4-PyS), 7.75 (d, 2H, μ-4-PyS), 7.98 (d, 1H, 2-PyS), 7.52 (t, 1H, 2-PyS), 6.80 (t, 1H, 2-PyS), 6.74 (d, 1H, 2-PyS), 1.73 (s, 15H, Cp^*), 1.83 (s, 15H, Cp^*). ^{13}C NMR (125 MHz, $CDCl_3$, ppm): δ 169.00, 150.42, 127.82 (4-PyS), δ 176.26, 145.77, 135.69, 130.58, 116.77 (2-PyS), 97.91, 94.16, 9.43, 9.18 (Cp^*). IR (KBr disk): ν = 3063, 2961, 2912, 1624, 1585, 1449, 1412, 1376, 1207, 1157, 1022, 819, 766, 725, 616, 581, 519 cm^{-1}.

4.8. Preparation of [Cp^*Rh(2-PyS)(μ-4-PyS)][Cp^*IrCl_2] (**9**)

The procedure is similar to the preparation of complex **8**. Using **6** (23 mg, 0.05 mmol) and **2** (20 mg, 0.025 mmol) to give **9** as an orange solid. Yield: 24 mg, 56%. Anal. Calc. for $C_{30}H_{38}N_2RhIrCl_2S_2$: C, 42.05; H, 4.47; N, 3.27. Found: C, 42.01; H, 4.52; N, 3.25%. ^{1}H NMR (500 MHz, $CDCl_3$, ppm): δ 8.49 (d, 2H, μ-4-PyS), 7.79 (d, 2H, μ-4-PyS), 7.93 (d, 1H, 2-PyS), 7.18 (t, 1H, 2-PyS), 6.79 (t, 1H, 2-PyS), 6.70 (d, 1H, 2-PyS), 1.78 (s, 15H, Cp^*), 1.80 (s, 15H, Cp^*). ^{13}C NMR (125 MHz, $CDCl_3$, ppm): δ 170.12, 148.95, 127.56 (4-PyS), δ 175.04, 145.35, 135.67, 129.51, 116.87 (2-PyS), 97.62, 94.40, 9.35, 9.12 (Cp^*). IR (KBr disk): ν = 3065, 2962, 2915, 1619, 1585, 1465, 1411, 1382, 1214, 1108, 1025, 911, 819, 727, 614, 507 cm^{-1}.

4.9. Preparation of Cp^*IrCl(2-PyS) (**11**)

A solution of *n*-BuLi (1.6 M, 0.32 ml, 0.5 mmol) in hexane was added dropwise to a solution of 2-mercaptopyridine (55 mg, 0.5 mmol) in 8 ml of THF at 0 °C. The suspension was stirred for another 1 h at room temperature. Then the solution was slowly added to a solution of **2** (200 mg, 0.25 mmol) in THF (20 ml) at −78 °C. After it had been stirred for one day, the solvent was removed under reduced pressure, and the residue was extracted with CH_2Cl_2. The filtrate was concentrated to about 5 ml and hexane was added, to give **11** as an orange solid. Yield: 187 mg, 79%. Anal. Calc. for $C_{15}H_{19}NIrClS$: C, 38.08; H, 4.05; N, 2.96. Found: C, 38.02; H, 4.16; N, 2.87%. ^{1}H NMR (500 MHz, $CDCl_3$, ppm): δ 8.58 (d, 1H, 2-PyS), 7.76 (t, 1H, 2-PyS), 6.78 (t, 1H, 2-PyS), 6.68 (d, 1H, 2-PyS), 1.71 (s, 15H, Cp^*). ^{13}C NMR (125 MHz, $CDCl_3$, ppm): δ 179.2, 146.6, 136.2, 128.2, 118.1 (PyS), 90.54, 10.19 (Cp^*). IR (KBr disk): ν = 3062, 1623, 1578, 1443, 1418, 1377, 1257, 1141, 1113, 1082, 1027, 765 cm^{-1}.

4.10. Crystal structure determinations

Diffraction data of complexes **3**, **4**·CH_2Cl_2, **6** and **11** were measured at room temperature on a Bruker SMART APEX CCD diffractometer with graphite-monochromated Mo Kα radiation (λ = 0.71073 Å). These structures were solved by the direct methods, and refined on F^2 by a full-matrix least-squares method (SHELXL) [27,28]. The non-hydrogen atoms were refined anisotropically and hydrogen atoms were included but not refined. Compound **3** crystallized with highly disordered interstitial solvent molecules. The diffuse electron density created by the interstitial molecules in **3** was analyzed using the program SQUEEZE in the PLATON software package [29]. Details of crystal data for complexes **3**, **4**·CH_2Cl_2, **6** and **11** are summarized in Table 1.

Acknowledgments

Financial support by the National Science Foundation of China (Grant No. 20871032), by Shanghai Leading Academic Discipline Project, Project No. B108 is gratefully acknowledged.

Appendix A. Supplementary material

CCDC 689381, 689380, 716885 and 716884 contain the supplementary crystallographic data for complexes **3**, **4**·CH_2Cl_2, **6** and **11**. These data can be obtained free of charge from The Cambridge Crystallographic Data Centre via www.ccdc.cam.ac.uk/data_request/cif. Supplementary data associated with this article can be

found, in the online version, at doi:10.1016/j.jorganchem.2009.05.034.

References

[1] K. Kitano, R. Tanaka, I. Kinoshita, K. Isobe, S. Ooi, J. Chem. Soc., Dalton Trans. (2000) 995.
[2] K. Umakoshi, A. Ichimurs, S. Ooi, Inorg. Chem. 29 (1990) 4005.
[3] L. Hao, R.J. Lachicotte, H.J. Gysling, R. Eisenberg, Inorg. Chem. 38 (1999) 4616.
[4] E.S. Raper, A.M. Britton, W. Clegg, J. Chem. Soc., Dalton Trans. (1990) 3341.
[5] M. El-khateeb, K. Damer, J. Organomet. Chem. 692 (2007) 2227.
[6] K. Ogata, A. Toyota, J. Organomet. Chem. 692 (2007) 4137.
[7] J. Martincova, L. Dosta, J. Tarab, A. Ruzicka, R. Jambor, J. Organomet. Chem. 692 (2007) 3415.
[8] Y.F. Han, Y.B. Huang, Y.J. Lin, G.X. Jin, Organometallics 27 (2008) 961.
[9] O.-K. Jung, Y.-A. Lee, Y.T. Kim, H.K. Chae, Inorg. Chim. Acta 299 (2000) 100.
[10] M. Kotera, Y. Sekioka, T. Suzuki, Inorg. Chem. 47 (2008) 3498.
[11] S. Liu, H. Wang, P.C. Zhang, L.H. Weng, X.F. Hou, Organometallics 27 (2008) 713.
[12] P.C. Zhang, H. Wang, S. Liu, X.Q. Guo, X.F. Hou, J. Organomet. Chem. 693 (2008) 2903.
[13] H. Wang, X.Q. Guo, R. Zhong, X.F. Hou, J. Organomet. Chem. 694 (2009) 1567.
[14] T. Habereder, W. Warcus, H. Nöth, K. Severin, Angew. Chem., Int. Ed. Engl. 38 (1999) 3225.
[15] H. Piotrowski, K. Polborn, G. Hilt, K. Severin, J. Am. Chem. Soc. 123 (2001) 2699.
[16] Z. Grote, R. Scopelliti, K. Severin, J. Am. Chem. Soc. 126 (2004) 16959.
[17] M.-L. Lehaire, R. Scopelliti, L. Herderis, K. Polborn, P. Mayer, K. Severin, Inorg. Chem. 43 (2004) 1609.
[18] T. Brasey, R. Scopelliti, K. Severin, Chem. Commun. (2006) 3308.
[19] D.P. Smith, M.T. Griffin, M.M. Olmstead, M.F. Maestre, R.H. Fish, Inorg. Chem. 32 (1993) 4677.
[20] H. Chen, M.M. Olmstead, D.P. Smith, M.F. Maestre, R.H. Fish, Angew. Chem., Int. Ed. Engl. 34 (1995) 1514.
[21] D. Carmona, F.J. Lahoz, R. Atencio, L.A. Oro, M.P. Lamata, F. Viguri, E. San José, C. Vega, J. Reyes, F. Joó, A. Kathó, Chem. Eur. J. 5 (1995) 1544.
[22] T. Poth, H. Paulus, H. Elias, C. Dücker-Benfer, R. van Eldik, Eur. J. Inorg. Chem. (2001) 1361.
[23] L. Mimassi, C. Guyard-Duhayon, M.N. Rager, H. Amouri, Inorg. Chem. 43 (2004) 6644.
[24] S. Ghosh, D.R. Turner, S.R. Batten, S. Mukherjee, Dalton Trans. (2007) 1869.
[25] Y.F. Han, Y.J. Lin, W.G. Jia, G.X. Jin, Dalton Trans. (2009) 2077.
[26] C. White, A. Yates, P.M. Maitlis, Inorg. Synth. 29 (1992) 228.
[27] SHELXTL 6.10, Bruker Analytical Instrumentation, Madison, WI, USA, 2000.
[28] G.M. Sheldrick, SADABS, Software for Empirical Adsorption Correction, University of Göttingen, Göttingen, Germany, 2000.
[29] A.L. Spek, J. Appl. Crystallogr. 36 (2003) 7.